



Corrosion Inhibition of Mild Steel in 200 ppm NaCl by the Addition of A Polymer

A Koulou^{*}, Y El Kaissi, N Errahmany, A Tazouti, A Rochdi, R Tourir, MS Elyoubi and M Ebn Touhami

Laboratory of Material Engineering and Environment: Modeling and Application, IBN Tofail University, Kenitra, Morocco

ABSTRACT

Our work was to develop new inhibiting formulations that meet the efficient, cost-effective and consistent with the restrictive environmental regulations. In this work, we studied the inhibition of corrosion of mild steel in 200 ppm NaCl by the addition of a sugar-based polymer. This study was carried out by various electrochemical, spectroscopic and surface analysis techniques. The results obtained show that this compound exhibits a better inhibitory efficiency which reaches 91% to 80 ppm and is dependent on the concentration, the temperature and the immersion time. The SEM-EDX analysis shows that the compound adsorbs to the metal surface.

Keywords: Adsorption; EIS; Polymeric corrosion inhibitor; Potentiodynamic polarization; Sodium chloride

INTRODUCTION

Among the problems of cooling water circuits are corrosion, scale and fouling by micro-organisms can occur when natural waters are used as thermal fluid. These problems have a major economic impact, since the first involves the deterioration of the metal surface, while the second leads to a loss of heat transfer capacity. These phenomena take place simultaneously in many industrial applications such as cooling systems, and therefore an investigation of their development and inhibition under real conditions becomes a subject of a large interest. Significant scientific and technological advances have been made to combat these phenomena, but they are still controlled by the addition of chemicals that inhibit their development. Various inhibitors have been used in cooling systems in order to solve these problems [1,2]. In particular, the fatty amine associated with phosphonocarboxylic acid salts was corrosion inhibitors standard [3]. Other researchers have focused their efforts on the synergy between molybdate and other organic and inorganic compounds for inhibiting corrosion and scale for the treatment of water in cooling circuits [4]. However, the use of heavy metal and corrosion inhibitors based on the inorganic compound are increasingly hampered by recent environmental restrictions. So inhibitors containing heavy metals are declining, due to concerns about their toxic effects [5]. Other surveys have been reported on gluconate and gluconic acid, as well as sodium, calcium and zinc salts of gluconic acid as successful inhibitors against corrosion of tin, iron and mild steel in media and almost neutral in simulated cooling water [6,7]. In response to environmental guidelines, this paper presents the effect of the addition of alkyl polyglucoside (APG) on the corrosion inhibition of mild steel in 200 ppm NaCl solution as simulating medium of natural water using polarization curves, electrochemical impedance spectroscopy, and gravimetric measurements as well as scanning electron microscopy. The impact of both addition of APG and biocide, namely cetyltrimethylammonium bromide (CTAB) was also investigated.

EXPERIMENTAL SECTION

Material Preparation

The working electrode was mild steel and its composition is summarized in Table 1. The Pt plate and saturated calomel were used as counter and reference electrode (SCE), respectively. All potentials are referred to this electrode. The corrosive solution is 200 ppm NaCl. This environment was chosen because its low conductivity is close to that of natural water used in the cooling circuits. The electrolyte was in contact with air without dissolved oxygen purge. The corrosion inhibitor studied in this work is the alkyl polyglucoside (APG). Its chemical formula is shown in Figure 1. It consists of a hydrophilic part of one or more glucose molecules and of the hydrocarbon chain which is the hydrophobic part. The APG belongs to the class of nonionic surfactants, sugar derivatives, natural (made from glucose and fatty alcohols), biodegradable and nontoxic. The biocide used in this study is cetyltrimethylammonium bromide (CTAB), the chemical structure of which is illustrated in Figure 1.

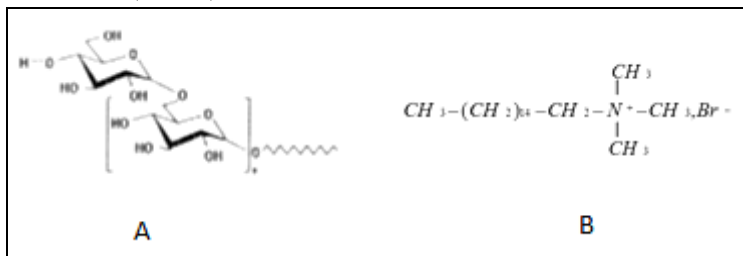


Figure 1: Chemical structure of APG (A) and CTAB (B)

Table 1: Chemical composition of mild steel

Element	Fe	C	Si	Mn	Cr	Mo	Ni	Al	Cu	Co	V	W
Weight (%)	98.7	0.11	0.24	0.47	0.12	0.02	0.1	0.03	0.14	<0.0012	<0.003	0.06

Weight Loss Measurements

Gravimetric measurements were performed as defined in the literature [8]. Mild steel samples used as corrosion test samples are rectangular (2.9 cm × 1.6 cm × 0.3 cm). After being abraded using emery paper (up to 1200 grade), cleaned with ethanol, washed with distilled water, dried and finally weighted, the samples were immersed for 4 h in 100 ml in non-inhibited and inhibited solutions at 295 K, controlled thermostatically and under an atmosphere of air. At the end of the experiments, the samples were cleaned according to ASTM G-81 and reweighed to 10⁻⁴ g to determine the corrosion rate [9]. The corrosion rate (C_R) and inhibition efficiency η_{WL} (%) were calculated according to the equations 1 and 2 [10,11] respectively:

$$C_R = \frac{W_b - W_a}{At} \quad (1)$$

$$\eta_{WL}(\%) = \left(1 - \frac{W_i}{W_o}\right) \times 100 \quad (2)$$

Where “ W_b ” and “ W_a ” are the sample weight before and after immersion in the tested solution, “ W_o ” and “ W_i ” are the values of corrosion weight losses of mild steel in the absence and presence of inhibitor, respectively, “ A ” the total area of the mild steel sample (cm²) and “ t ” is the exposure time (h).

Polarization Measurements

The working electrode was immersed in the solution for 1 h until an open circuit potential at steady state (E_{OCP}). Cathodic polarization was recorded by E_{OCP} in negative direction of polarization potentiodynamic conditions corresponding to 1 mVs⁻¹ (scanning speed) and under air atmosphere. After this sweep, the anodic polarization was recorded by polarization E_{OCP} in the positive direction. The potentiodynamic measurements were performed using a potentiostat type VoltaLab PGZ 100, controlled by a personal computer. As the conductivity of the medium studied is small, the polarization curves $J(E)$ have been corrected from the ohmic drop $R_S J$. The solution resistance, R_S , was deducted by electrochemical impedance spectroscopy below. On the Nyquist diagrams, R_S is the abscissa of the intersection of high-frequency diagram with the real axis.

The evaluation parameters of the corrosion kinetics was determined by fitting using the Stern-Geary equation. The inhibitory efficacy was evaluated from the measured J_{corr} values using the relationship:

$$\text{IE}\% = \frac{J_{\text{corr}}^0 - J_{\text{corr}}}{J_{\text{corr}}^0} \times 100 \quad (3)$$

where J_{corr}^0 and J_{corr} are the corrosion current densities values in the absence and the presence of inhibitor, respectively.

Electrochemical Impedance Spectroscopy Measurements

The electrochemical impedance spectroscopy measurements were carried out using a transfer function analyser (VoltaLab PGZ 100), with a small amplitude ac. signal (10 mV rms), over a frequency domain from 100 kHz to 10 mHz at 295 K and in air atmosphere. The results were then analysed in terms of equivalent electrical circuit using Bouckamp program [12]. The polarization resistance R_p , is obtained from the diameter of the semicircle in the Nyquist representation. The inhibition efficiency of the studied inhibitor has been found from the relationship:

$$\text{IE}\% = \frac{R_p - R_p^0}{R_p} \times 100 \quad (4)$$

Where R_p^0 and R_p are the polarization resistance values without and with inhibitor, respectively.

Scanning Electron Microscopy (SEM)

Surface examination of mild steel after exposure to 200 ppm NaCl solution with and without the inhibitor was carried out using scanning electronic microscope (SEM, JOEL JSM5500).

RESULTS AND DISCUSSION

Gravimetric Study

Effect of APG concentration:

The effect of addition of APG tested at different concentrations on the corrosion of mild steel in 200 ppm NaCl solution was studied by weight loss method at 295 K after 4 h of immersion period.

Table 2: Corrosion weight loss of mild steel in 200 ppm NaCl in presence and absence of apg for 4 h

Concentration ppm	C_R ($\text{mg}\cdot\text{cm}^{-2}\cdot\text{h}^{-1}$)	η_{WL} (%)
Blank	0.027	-
10	0.017	36
20	0.015	45
40	0.01	64
80	0.005	82
100	0.007	73
120	0.012	55

The obtained values of corrosion rate (C_R) and inhibition efficiency $\eta_{\text{WL}}(\%)$ are summarized in Table 2. It is obvious from these results that the APG inhibits the corrosion of mild steel at all concentrations used in this study. The variation of C_R and $\eta_{\text{WL}}(\%)$ with the APG concentration are shown in Figure 2. It can be observed from this figure, that the C_R of mild steel decreases while the protection efficiency increases as the APG concentration increases in 200 ppm NaCl solutions. This conclusion was also supported by the electrochemical studies reported below. The maximum $\eta_{\text{WL}}(\%)$ of 82% is achieved at 80 ppm and a further increase in concentration did not cause any appreciable change in the performance of the inhibitor. This behavior could be attributed to a strong interaction by adsorption between the compound and the metal surface [13]. This may also be due to the adsorption of the inhibitor to the surface of the mild steel through pairs of non-binding electrons present on the nitrogen, oxygen and sulfur atoms as well as on the π electrons [14]. Other authors have shown that the molecular surface [15] and the molecular

weight [16] of the organic molecule have an effect on the inhibition of metal corrosion. However, inhibition efficiency depends mainly on the -OH group in APG. The mono-electron pair on oxygen will coordinate with the metal atoms of the active sites, causing a stronger interaction with the metal surface, and it has been found that $\eta_{WL}(\%)$ increases with electron density. The oxygen atom can give π electrons to the surface of the metal and increase the adsorption and hence a higher inhibition efficiency.

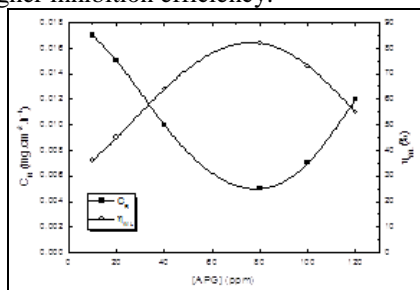


Figure 2: The variation of C_R and $\eta_{WL}(\%)$ with the APG concentration

Effect of immersion time:

The effect of immersion time on the $\eta_{WL}(\%)$ of APG for mild steel corrosion in 200 ppm NaCl, was studied by immersing the steel specimen in 80 ppm inhibited chloride solution for exposure period extending up to 25 h at 295 K and the results are produced in Figure 3.

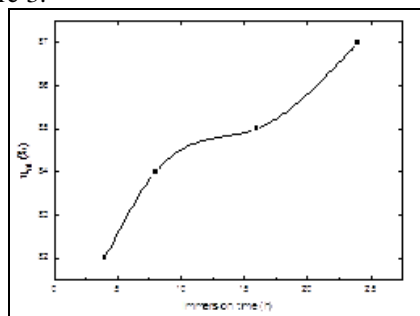


Figure 3: Influence of immersion time on the efficacy of APG at 80 ppm

We note that the inhibition efficiency increases with increasing immersion time, reaching a maximum after 25 h. This result can be explained by the thickening of the film formed.

Effect of temperature:

In order to study the effect of temperature on the corrosion inhibition property of the APG, gravimetric experiments were conducted in the range of 295-325 K, in the absence and presence of 80 ppm of inhibitor. The analysis of the obtained data, collected in Table 3, clearly shows an increase of corrosion rate (C_R) with the rise of temperature and it is more pronounced for uninhibited solution (200 ppm NaCl). We also note that the inhibition efficiency depends on the temperature and decreases with the rise of temperature from 295 to 325 K, indicating that higher temperature dissolution of mild steel predominates on adsorption of APG at the metal surface. This can be explained by the decrease of the strength of the adsorption process at high temperature, and can suggest a physical adsorption mode (Figure 4).

	Temperature (K)	$C_{R \text{ mg.cm}^{-2}.\text{h}^{-1}}$	$\eta_{WL}(\%)$
Blank	295	0.027	-
	305	0.035	-
	315	0.105	-
	325	0.16	-
	295	0.005	82
80 ppm APG	305	0.018	50
	315	0.06	43
	325	0.105	34

Table 3: Corrosion weight loss of mild steel in 200 ppm NaCl with and without 80 ppm of APG at various temperatures

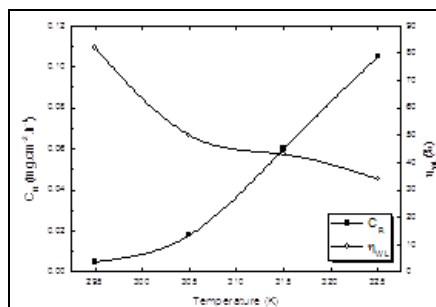


Figure 4: The variation of CR and η_{WL} (%) at different temperatures for 80 ppm of APG

In order to calculate activation thermodynamic parameters of the corrosion process, Arrhenius E_a (5) used [17]:

$$C_R = A \exp\left(-\frac{E_a}{RT}\right) \quad (5)$$

Where, E_a is the apparent activation corrosion energy, R is the universal gas constant, A is the Arrhenius pre-exponential factor. Arrhenius plots for the corrosion rate of mild steel are plotted in Figure 5. Values of apparent activation energy of corrosion (E_a) were determined from the slope of $\ln(C_R)$ vs. $1000/T$ plots. These plots are straight lines and the slope of each one gives its activation energy E_a . It is observed that for the mild steel corrosion in 200 ppm NaCl solution, the E_a value was found equal to $53.47 \text{ kJ}\cdot\text{mol}^{-1}$. In the presence of APG, the E_a value is higher and equal to $85.89 \text{ kJ}\cdot\text{mol}^{-1}$. According to Gomma [18], the kinetics of such corrosion process acquires the character of a diffusion process in which at lower temperature the quantity of inhibitor present at the metal surface is greater than that at higher temperatures. However, the negative slope of Arrhenius coordinates indicates that the organic compounds are adsorbed on metallic surface [19].

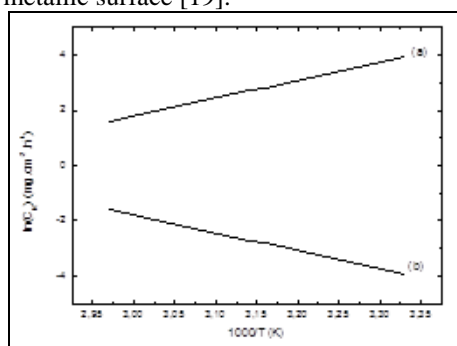


Figure 5: Variation of the rate of corrosion as a function of the reciprocal of the temperature: (a) in the absence of the inhibitor; (B) with 80 ppm of APG

Effect of CTAB addition:

We examined the effect of adding a non-oxidizing biocide CTAB on the inhibition efficiency of APG. We recall that the CTAB is used to decrease biological fouling. For example, previous studies have shown that this biocide has very good inhibition efficiency against bacterial growth when added at 15 ppm of concentration [20,21]. For this purpose, we tested the effect of this biocide.

Table 4: Corrosion weight loss of mild steel in 200 ppm NaCl containing 15 ppm of CTAB and 15 ppm of CTAB + 80 ppm of APG

Concentration ppm	C_R mg.cm ⁻² .h ⁻¹	η_{WL} (%)
Blank	0.027	-
15 CTAB	0.008	70
80 APG + 15 CTAB	0.015	45

Table 4 shows the results of the effect of adding CTAB biocide on the APG inhibitory efficiency. It is note that the CTAB appears like a corrosion inhibitor and has inhibition efficiency about 70%. This result is in agreement with literature work [20,22]. However, the addition of CTAB largely affects the efficiency of APG. This shows that it does not have a synergistic effect between the two compounds.

Potentiodynamic Polarization Study

The plot of the polarization curve of the steel in the 200 ppm NaCl solution was carried out in potentiostatic mode. Before any manipulation, the electrode is kept immersed for 4 hours at the corrosion potential. This time is necessary to make the system tend to a steady state. We have adopted this procedure to get as close as possible to the actual operating conditions of the electrode and taking into account corrosion products. The polarization curves obtained for the mild steel in the presence and absence of the APG inhibitor are shown in Figure 6 after 4 hours of immersion in the 200 ppm NaCl solution at a rotation speed of 1000 rpm and a scanning speed of 1 mV.s⁻¹.

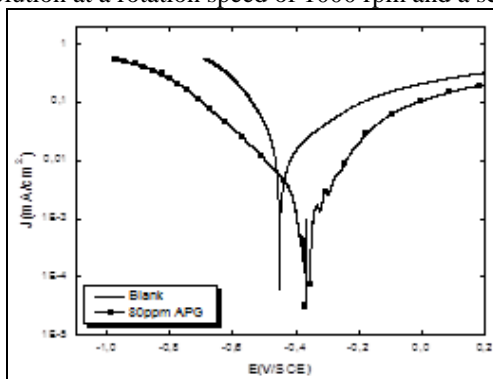
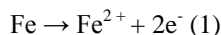


Figure 6: Polarization curves of mild steel in 200 ppm NaCl solution at 80 ppm of APG

In the absence of the inhibitor and in the anodic domain, the exponential rate shows that the iron oxidation process is governed by pure charge transfer kinetics. The reaction involved is as follows:



Thus, the corrosion current density obtained from the extrapolation of the Tafel line is of the order of 12 $\mu\text{A}\cdot\text{cm}^{-2}$. The addition of APG to the corrosive solution displaces the corrosion potential (E_{corr}) to more anodic potentials. This displacement is about 100 mV/SCE in the presence of 80 ppm in inhibitor so the densities of the anode and cathodic current decreases significantly. This makes it possible to conclude that APG is a mixed inhibitor.

Table 5: Electrochemical parameters from the polarization curves in absence and presence of 80 ppm of APG

Concentration ppm	E_{corr} mV/SCE	J_{corr} $\mu\text{A}\cdot\text{cm}^{-2}$	IE%
Blank	-454	12	-
80 APG	-354	1.2	90

Analysis of the results obtained (Table 5) shows that the density of the corrosion current J_{corr} decreases remarkably in the presence of 80 ppm as inhibitor. At this concentration, the inhibitory efficiency is of the order of 90%. This can be explained in general by the blocking of the active sites by the formation of a protective layer on the surface of the sample. Figure 7 shows the effect of temperature was achieved by the polarization curves plotted at different temperatures in the presence of 80 ppm of APG. Examination of these curves shows that the increase in temperature hardly affects their general shape and shifts the corrosion potential to more negative values (Table 3). 6 summarizes the electrochemical parameters associated with these curves.

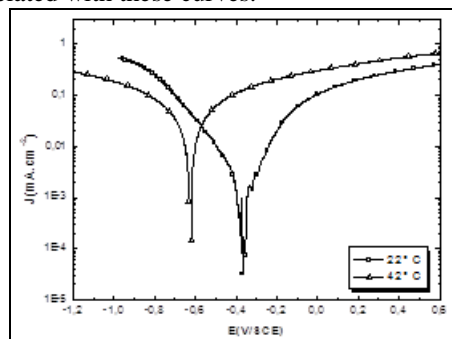


Figure 7: Polarization curves of mild steel in a 200 ppm NaCl solution at different temperatures and in the presence of 80 ppm of APG

We note that the corrosion current density increases substantially with the increase of the temperature in the absence and in the presence of inhibitor. This confirms the increase in the corrosion kinetics of the steel with this parameter. The inhibitor efficiency experienced a remarkable drop in temperature increase. This effect is attributed to the increase in the amount of oxygen scattered, with increasing temperature. Figures 8 and 9 show the polarization curves for the behavior of mild steel in 200 ppm NaCl solution in the absence, in the presence of 15 ppm CTAB and in the presence of 80 ppm APG with 15 ppm CTAB after 4 hours of immersion.

Table 6: Electrochemical parameters from the polarization curves in the presence of 15 ppm of CTAB

Concentration ppm	E_{corr} mV/SCE	J_{corr} $\mu\text{A.cm}^{-2}$	I_{ev}
Blank	-454	12	-
15 CTAB	-500	6	50

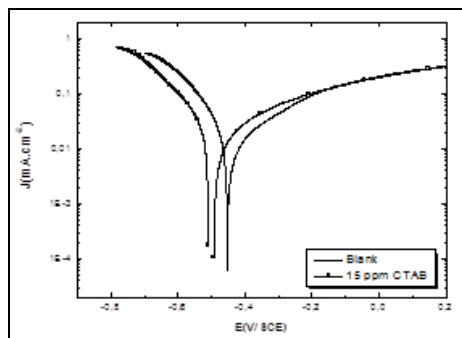


Figure 8: Polarization curves of mild steel in 200 ppm NaCl solution in the presence of 15 ppm CTAB

The addition of the biocide alone to the corrosive solution displaces the corrosion potential towards the more cathodic values and lowers the cathodic current densities. This makes it possible to conclude that the biocide used behaves as a cathodic corrosion inhibitor. Thus the inhibitory efficacy is of the order of 50% to 15 ppm of CTAB. Table 6 gives the electrochemical parameters associated with these curves (Figure 9).

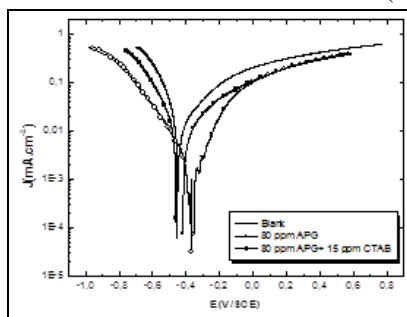


Figure 9: Polarization curves of mild steel in 200 ppm NaCl solution in the presence of APG and CTAB

In the presence of the mixture the current densities are higher than those obtained in the presence of APG alone and consequently the addition of CTAB affects the effectiveness of the inhibitor. The electrochemical parameters are illustrated in Table 7.

Table 7: Electrochemical parameters resulting from the polarization curves in the presence of the inhibitor and of the biocide

Concentration ppm	E_{corr} mV/SCE	J_{corr} $\mu\text{A.cm}^{-2}$	IE%
Blank	-454	12	-
80	-354	1.2	90
80 APG + 15 CTAB	-458	5.8	51

Electrochemical Impedance Spectroscopy (EIS)

The electrochemical impedance diagrams obtained at the corrosion potential after 4 hours of immersion in absence and in the presence of 80 ppm as inhibitor are presented in Figure 10.

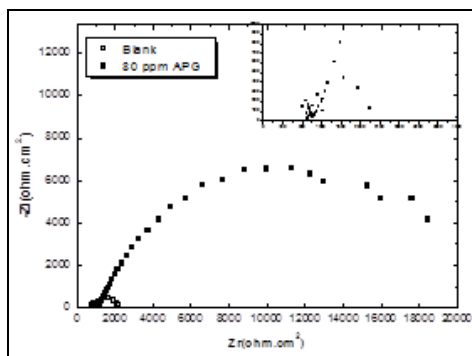


Figure 10: Polarization curves of mild steel in 200 ppm NaCl solution in the presence of APG and CTAB

We note that the addition of the inhibitor does not affect the general appearance of the impedance curves. We also see a strong increase in the size of the loop and therefore an increase of the polarization resistance which is inversely proportional to the corrosion rate. This result reflects the influence of the inhibitor on the process at the mild steel / solution interface. The electrochemical parameters are recorded in Table 8. Examination of this table shows a decrease in the capacity of the double layer, it passes from $283 \mu\text{F}\cdot\text{cm}^{-2}$ to $158 \mu\text{F}\cdot\text{cm}^{-2}$ to 80 ppm as inhibitor. This can be explained by the gradual replacement of water and / or hydroxyl molecules by the APG molecules on the metal surface indicating the decrease of the active sites of the metal dissolution reaction. In accordance with the stationary electrochemical results, the impedance measurements perfectly confirm the high protective power of the APG at a low concentration of 80 ppm.

Table 8: Electrochemical parameters derived from the electrochemical impedance diagrams detected at the corrosion potential at 80 ppm APG

Concentration ppm	R_S ohm.cm ²	R_P ohm.cm ²	C_{dl} $\mu\text{F}\cdot\text{cm}^{-2}$	IE%
Témoin	920	1780	283	-
80 APG	1017	20131	158	91

Figure 11 shows the electrochemical impedance diagrams obtained at the corrosion potential after 4 hours of immersion in the absence and presence of 80 ppm as inhibitor and of the biocide. In the presence of the inhibitor and the biocide, we note that the polarization resistance becomes weaker than that obtained in the presence of APG alone, which makes it possible to say that the addition of the CTAB significantly reduces the efficiency of the anti-inhibitor. The electrochemical parameters are given in Table 9.

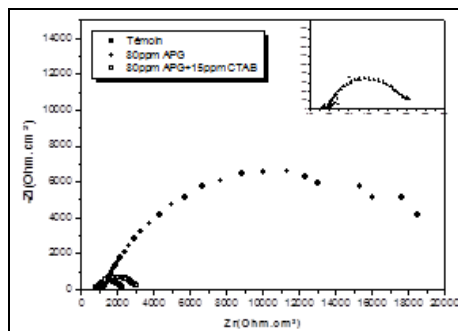


Figure 11: Diagrams of electrochemical impedance measured at the corrosion potential in the presence of the inhibitor and the biocide

Table 9: Electrochemical parameters derived from the electrochemical impedance diagrams detected at the corrosion potential in the presence of monomer and biocide

Concentration ppm	R_S ohm.cm ²	R_P ohm.cm ²	C_{dl} $\mu\text{F}\cdot\text{cm}^{-2}$	IE%
Témoin	920	1780	283	-
80 APG	1017	20131	158	90
80 APG + 15 CTAB	890	2380	211	26

The electrochemical impedance measurements perfectly confirm the results obtained by the gravimetric method and the polarization curves.

Scanning Electron Microscopy, SEM Analyses

The determination of the nature of the film thus formed on the surface of the steel was carried out by observation using a scanning electron microscope (Figure 12).

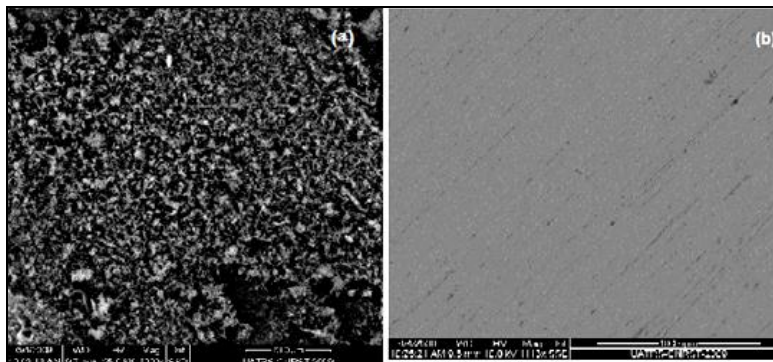


Figure 12: Morphology of the electrode surface of mild steel immersed in the 200 ppm NaCl solution for 24h of immersion: (a) in the absence of inhibitor (b) in the presence of 80 ppm APG

In the absence of an inhibitor, the oxide layer developed on the surface of the steel is not homogeneous having a filamentous deposit. The EDX analysis carried out on this zone reveals the presence of oxygen and iron (Figure 13). This is likely to correspond to the structure of an iron oxide / hydroxide compound. In the presence of an inhibitor, it is clear that the APG compound significantly improves the surface condition of the immersed steel for 24 hours in the corrosive solution. The qualitative analysis by EDX (Figure 14) reveals peaks relative to carbon and oxygen which are the main constituents of APG, thus indicating the adsorption of this compound on the surface of mild steel. Thus observation by scanning electron microscope perfectly confirms the results obtained by the gravimetric measurements and the stationary and transient electrochemical tests.

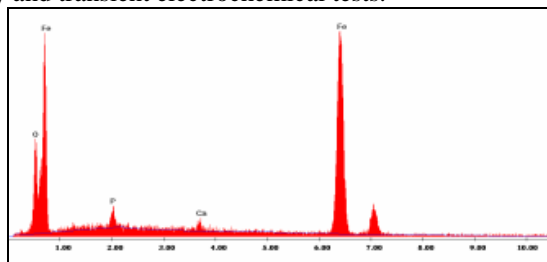


Figure 13: Qualitative EDX of the surface state of mild steel after immersion in 200 ppm NaCl solution for 24 hours

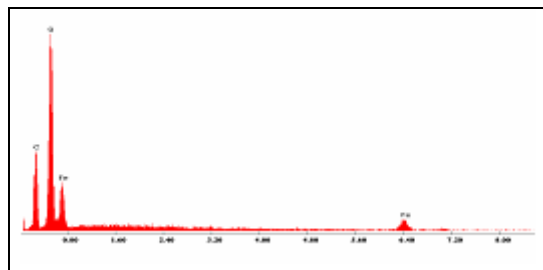


Figure 14: Qualitative EDX of the surface condition of mild steel after immersion in 200 ppm NaCl solution containing 80 ppm of APG for 24 hours

CONCLUSION

During this work, we made a contribution to the study of the protection of mild steel in a 200 ppm sodium chloride solution. First, the gravimetric and electrochemical studies by plotting the IE curves confirm that the 200 ppm

sodium chloride solution is slightly aggressive. Indeed, the surface state of the electrode, after immersion in the corrosive solution, has a layer of corrosion product, and the corrosion rate is of the order of $12 \mu\text{A}\cdot\text{cm}^{-2}$. The study of the inhibition of the corrosion of mild steel in the waters of the cooling circuits concerned a novel corrosion inhibitor which is alkyl polyglucoside (APG). The results obtained show that this compound is a mixed inhibitor and exhibits an inhibitory efficiency of the order of 90%. The latter improves with immersion time, and decreases greatly with temperature and with the addition of the biocide.

REFERENCES

- [1] LL Sheir, RA Jarman. Corrosion, third edition, Butterworth-Heinmann Ltd., Great Britain, **1994**.
- [2] DA Jones. Principles and Prevention of Corrosion, Macmillan Publishing Company, USA, **1991**.
- [3] N Ochoa; G Baril; F Moran; N Pébère. *J Appl Electrochem.* **2002**, 32, 497.
- [4] RW Flynn, MJ Grouke. *US Patent 4.* **1981**, 243, 316.
- [5] DL Lake. Corrosion Prevention and Control, **1988**, 113.
- [6] PR Puckorius; SD Strauss. *Power.* **1995**, 5, 17.
- [7] MA Pech-Canul; LP Chi-Canul. *Corros Sci.* **1999**, 55, 948.
- [8] I Sekine; M Sanbongi; H Hagiuda; T Oschibe; M Yuasa; T Imahama; Y Shibata; T Wake. *J Electrochem Soc.* **1992**, 139, 3167.
- [9] ASTM G-81, Annual Book of ASTM Standards, **1995**.
- [10] I Ahamad; R Prasad; MA Quraishi. *Corros Sci.* **2010**, 52, 933-942.
- [11] F Bentiss; M Outirite; M. Traisnel; H Vezin; M Lagrenée; B Hammouti; SS Al Deyab; C Jama. *Int J Electrochem Sci.* **2012**, 7, 1699-1723.
- [12] A Bouckamp, Users Manual Equivalent Circuit, Ver, **1993**, 4, 51.
- [13] RS Chaudhary; S Sharma. *Indian J Chem Technol.* **1999**, 6, 202.
- [14] F Bentiss; M Traisnel; M Lagrenée. *Appl Surf Sci.* **2000**, 161, 196.
- [15] MA Quraishi; D Jamal. *Mater Chem Phys.* **2003**, 78, 608.
- [16] MA Quraishi; HK Sharma. *Mater Chem Phys.* **2002**, 78, 18.
- [17] JOM Bockris; AKN Reddy. Modern Electrochemistry, Plenum Press, New York, **1977**, 2.
- [18] GK Gomma. *Mat Chem Phys.* **1998**, 56, 27.
- [19] M Bouklah; B Hammouti; M Lagrenée; F Bentiss. *Corros Sci.* **2006**, 48, 2831.
- [20] S Ramesh; S Rajeswari; S Maruthamuthu. *Mater Lett.* **2003**, 57, 4547.
- [21] S Ramesh; S Rajeswari. *Corros Sci.* **2005**, 47, 151.
- [22] R Touir; N Dkhireche; M Ebn Touhami; M El Bakri; A Rochdi; RA Belakhmima. *J Saudi Chem Soc.* **2011**.